J Mater Sci: Mater Electron (2013) 24:2750–2754
DOI 10.1007/s10854-013-1165-7

Band gap broadening and photoluminescence properties investigation in Ga_2O_3 polycrystal

Yi Cheng · Hongwei Liang · Rensheng Shen · Xiaochuan Xia · Bo Wang · Yuanda Liu · Shiwei Song · Yang Liu · Zhenzhong Zhang · Guotong Du

Received: 3 January 2013 / Accepted: 26 February 2013 / Published online: 9 March 2013

Abstract Ga_2O_3 thin films were deposited on c-plane Al_2O_3 substrates by electron beam evaporation equipment. The effects of post anneal treatment on structure and optical properties of Ga_2O_3 were investigated. The X-ray diffraction (XRD) results of the as-grown and the annealed samples indicated the films consisted with the mix of β-phase polycrystalline and amorphous Ga_2O_3. The electron diffraction pattern confirmed the existence of the nanocrystal grains. AFM images revealed that the anneal treatment promoted the film crystallization. Both Ga_2O_3 fims exhibited high transparency from visible light to near infrared region. An obvious band gap broadening phenomenon was observed for the annealed sample comparing with the as-grown sample. The optical band gap of the annealed sample was as large as 5.68 eV, which was inconsistent with the bulk β-phase Ga_2O_3. Meanwhile, the center of ultraviolet emission peak blue shifted about 0.42 eV for the annealed samples. The mechanism of the band gap broadening effect and ultraviolet emission peak blue shift were discussed.

Y. Cheng · H. Liang (✉) · R. Shen · X. Xia · B. Wang · Y. Liu · S. Song · Y. Liu · G. Du
School of Physics and Optoelectronic Engineering, Dalian University of Technology, Dalian 116024, People's Republic of China
e-mail: hwliang@dlut.edu.cn

Y. Cheng
Department of Physics, Dalian Maritime University, Dalian 116026, People's Republic of China

Z. Zhang
State Key Laboratory of Luminescence and Applications, Changchun Institute of Optics Fine Mechanics and Physics, Chinese Academy of Sciences, Changchun 130033, People's Republic of China

G. Du (✉)
State Key Laboratory on Integrated Optoelectronics, College of Electronic Science and Engineering, Jilin University, Changchun 130023, People's Republic of China
e-mail: dugt@dlut.edu.cn

1 Introduction

Recently Ga_2O_3 is regarded as the novel and promising candidate for optoelectronic devices, due to its wide direct band gap of 4.9 eV [1, 2]. As reported, the Ga_2O_3 film had a variety of applications, such as ultraviolet photodetectors [3], light emitting diodes [4], field effect transistors and transparent conductive devices [5, 6]. Especially, it has great potential application in fabricating solar blind photodiodes [7, 8]. Thus, investigating the optical properties of the Ga_2O_3 film, and analyzing the Ga_2O_3 crystalline structure become necessary and important. The Ga_2O_3 films have been prepared by several methods such as molecular beam epitaxy (MBE) [9], sputtering [10], pulsed laser deposition (PLD) [11], metal–organic chemical vapor deposition (MOCVD) [12] and electron beam evaporation [13]. Among them, electron beam evaporation possessed the advantages of depositing high quality films due to its efficient, low cost, convenient and high growth rate.

As well known, thermal treatment in different gas ambient was an effective and convenient strategy to change the optical properties of films. Because high temperature anneal treat could make surface absorb impurities or change chemical composition ratio of the films, in previous works [14], we studied the effect of annealing treatment on the crystalline quality and optical properties in N_2 ambient. As well, high temperature provided enough energy to the atoms on the substrate, so that it increased their surface

mobility and made the O and Ga atoms in the right lattice position. However, the as-grown Ga_2O_3 films resided oxygen vacancies, gallium vacancies and gallium- oxygen vacancies pairs intrinsic defects. Rich oxygen anneal treatment could optimize the chemical composition ratio of Ga atom and O atom. In order to further research the influence of anneal treatment ambient on the optical band gap of the amorphous or polycrystalline Ga_2O_3 films, the as-grown films were annealed in O_2 ambient at 1,000 °C for 1 h. Then the crystal structure, photoluminescence properties and the optical band gap of Ga_2O_3 were discussed in details.

2 Experiments

Using electron beam evaporation equipment, Ga_2O_3 films were deposited on c-plane Al_2O_3 substrate. The Ga_2O_3 ceramic target was sintered at 1,550 °C for several hours with high-purity (99.99 %) Ga_2O_3 powder. Before growth, the c-plane Al_2O_3 substrates were sequentially degreased in ultrasonic baths of acetone, ethanol and deionized water for 5 min, respectively. The substrates were not heated and kept at about 150 mm away from the target. The background vacuum pressure of the growth chamber was about 4×10^{-3} Pa before depositing Ga_2O_3 films. The voltage of electron beam evaporation source was 6 kV. The samples thicknesses were about 200 nm, which was monitored by the films thickness monitor (CRTM-6000). In order to investigate the film crystalline quality and optical properties affected by post thermal treatment, the as-grown β-Ga_2O_3 sample was subsequently annealed at 1,000 °C under oxygen ambient for 1 h.

The crystalline properties were investigated by Panalytical Empyrean X-ray diffraction (XRD) instrument. The photoluminescence (PL) spectra were measured by a He-Ag deep ultraviolet laser (224 nm, 50 mW) with the Andor idus DU420A photo detector. The optical transmission and absorption spectra were recorded by Shimadzu UV3600 spectrometer. All the measurements were performed at room temperature (RT).

3 Results and discussion

Figure 1 presented the XRD patterns of the as-grown and the annealed samples. The main diffraction peaks in the patterns can be indexed to a monoclinic structure, which is good agreement with bulk β-Ga_2O_3 crystals structure patterns of JCPDS-pdf, No.43-1012. No appreciable diffraction peaks corresponding to other Ga_2O_3 polymorphs were observed either in the as-grown and the annealed samples. XRD patterns indicated that both samples distributed ploycrystalline β-Ga_2O_3 and amorphous Ga_2O_3, in terms of the various diffraction peaks and the distinct envelope centered at 19.0 degree. Therefore, the physical model of the structure could be viewed as various nanocrystal grains embedded in a matrix of amorphous Ga_2O_3 thin film. Next, the electron diffraction pattern confirmed the existence of the nanocrystal grains. To further investigate the effect of O_2 anneal treatment on the structure of Ga_2O_3 films, the surface morphologies of as-grown and annealed samples were observed by AFM images.

Figure 2 showed the AFM images of surface morphologies for a $5\mu m \times 5\mu m$ scanning area of as-grown and annealed samples. After anneal treatment, the surface morphologies became rough, and the grain size enlarged. The root mean square (RMS) surface roughness of the as-grown and annealed samples increased, which were 4.01 and 6.30 nm. Figure 2(b) revealed that high temperature O_2 anneal treatment made the Ga_2O_3 films surface morphology much rough than the as-grown samples. Same with the XRD results, it again indicated that the O_2 participated in the Ga_2O_3 films with preferred orientation deposition. Oxygen anneal treatment optimized the chemical composition ratio of Ga atom and O atom. Hence, anneal treatment promoted the Ga_2O_3 films crystallization.

The nanocrystal grains embedded in annealed Ga_2O_3 film were further examined using high-resolution transmission electron microscopy (HRTEM). Figure 3(a) showed the cross-sectional HRTEM micrograph of the undoped Ga_2O_3/sapphire structure. The interfaces of Ga_2O_3 and sapphire could be clearly identified. The incident electron beam was parallel to the $[1\bar{1}00]$ direction of c-plane Al_2O_3. The interplanar d-spacing of Ga_2O_3 was about 0.44 nm, indexed to the β phase $Ga_2O_3(\bar{2}01)$ plane. The d-spacing of sapphire was 0.35 nm, indexed to the c-plane

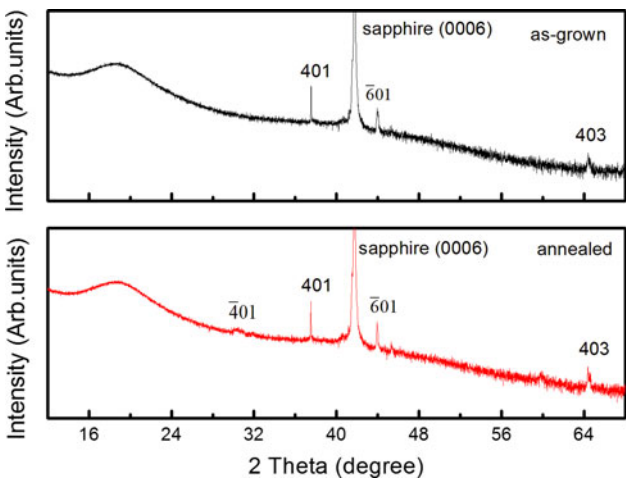

Fig. 1 XRD patterns of as-grown and annealed Ga_2O_3 films

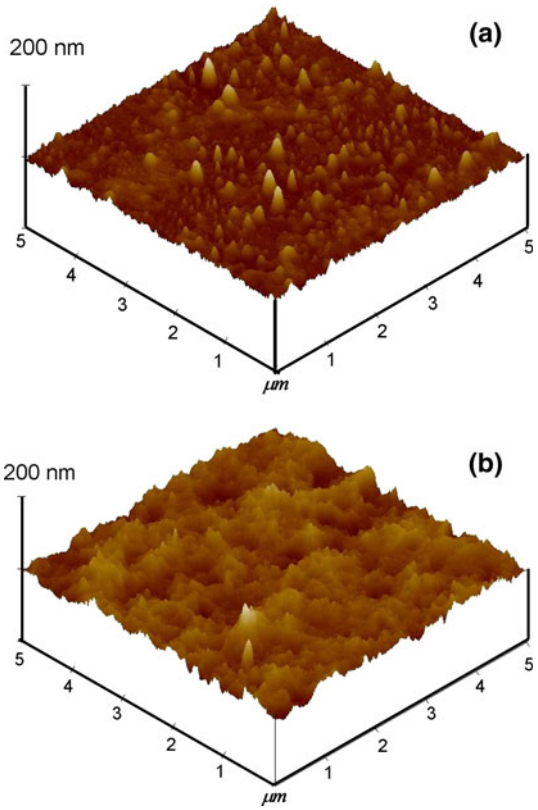

Fig. 2 AFM images of the as-grown and annealed Ga_2O_3 films **a** as-grown **b** annealed

$Al_2O_3(012)$ plane. To improve the nanocrystal grains embedding in the Ga_2O_3 film, the associated selected area of electron diffraction (SAED) pattern was presented in Fig. 2(b). The diffuse electron diffraction rings patterns revealed the microcrystal properties of the films.

Figure 4 showed photoluminescence spectra of c-plane Al_2O_3 substrate, as-grown and annealed Ga_2O_3 samples. The excitation wavelength of photoluminescence spectra is 224 nm. For annealed sample, two broad emission peaks centered at 330 nm (3.76 eV) and 706 nm (1.76 eV) were observed. However, it was not detected obvious photoluminescence in as-grown sample. Meanwhile, the near band edge (NBE) emissions of Ga_2O_3 were not detected in both samples. As reported, the broad ultraviolet (UV) emission centered at 330 nm was caused by the localization of recombining electrons and holes [15]. Comparing with bulk single crystal β-Ga_2O_3 [16, 17], the center of UV emission peak blue shifted about 0.42 eV for the annealed samples. The phenomena further confirmed that nanocrystal grains embedded in amorphous Ga_2O_3 thin film. As well known, if the nanocrystal grains sizes were less than the exciton Bohr radius, it would cause quantum effect [18]. Generally, quantum confinement effect shifts the energy levels of the conduction and valence bands apart, giving rise to a blue shift in the transition energy with the particle size decreasing [19, 20]. Same phenomenon was also revealed in the calculated optical band gap.

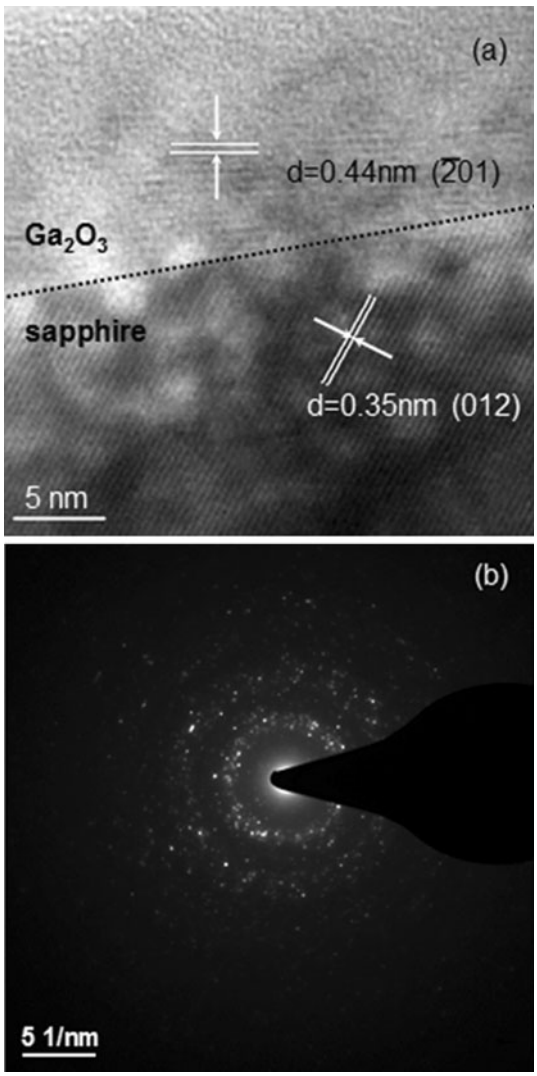

Fig. 3 Cross-sectional high resolution TEM images and the SEAD patterns of annealed Ga_2O_3 film **a** high resolution TEM images **b** SEAD patterns

The nature of the PL of Ga_2O_3 was still a matter of controversy. Three mechanisms had been presented to explain the UV emission of Ga_2O_3 films [21, 22]. In our case, the UV emission was attributed to the recombination of gallium vacancies and oxygen vacancies or gallium-oxygen vacancy pairs, and the broad red emission was due to intrinsic impurities. In addition, the peaks at 448 and 672 nm were the laser frequency doubling peaks. It is reported that the NBE emissions of β-Ga_2O_3 of the monoclinic phase is 265 nm (4.6 eV) and 278 nm (4.5 eV) [23]. But in our experiment, it had not been found. In order to estimate the energy band gap of the Ga_2O_3 sample, we introduced the absorption measurement to calculate the optical band gaps.

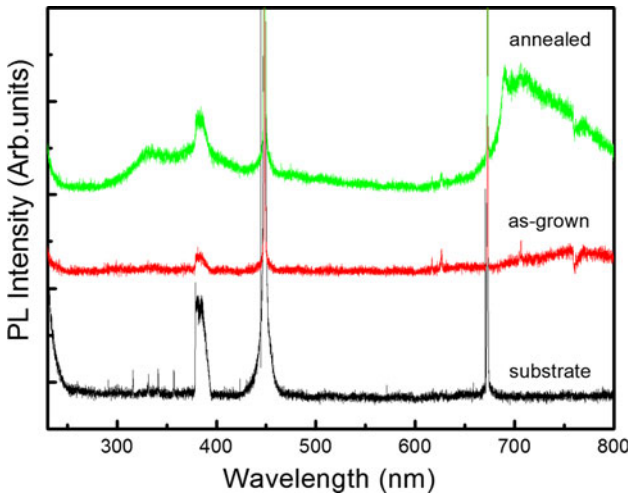

Fig. 4 Room temperature PL spectra of substrate, as-grown and annealed Ga_2O_3 films

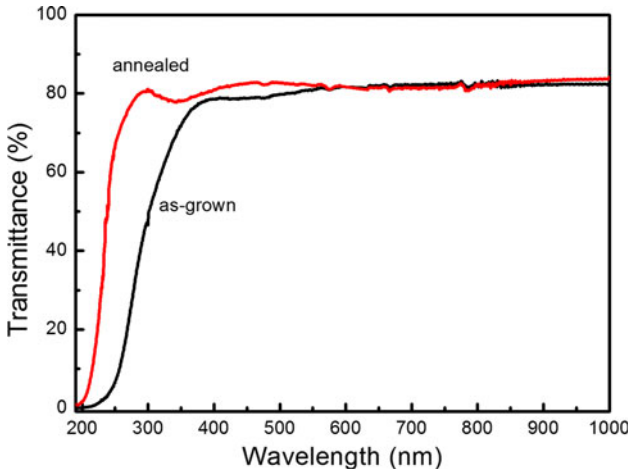

Fig. 5 Room temperature transmittance spectra of as-grown and annealed Ga_2O_3 samples

Figure 5 illustrated that the as-grown and annealed samples exhibited high transparency in visible light and near infrared region with transmittance about 80 %. Meanwhile, the absorption edge was a slightly moved toward short wavelength for the annealed samples. It might be caused by increasing quantity of nanocrystal.

Ga_2O_3 is direct band gap materials, which optical band gap could be deduced from absorption spectra. It exists the relation $\alpha hv = A(hv - E_g)^{1/2}$, whereas $(\alpha hv)^2$ is plotted versus photon energy hv. A is the constant, E_g is the optical band gap, and α is the absorption coefficient. Through linear extrapolating to zero, where absorption coefficient α equals zero $(\alpha = 0)$, then the optical band gap value could be obtained. In terms of the absorbing spectra of the as-grown and annealed samples, we obtained the $(\alpha hv)^2$ versus photon energy (hv) curves, as shown in Fig. 6. The

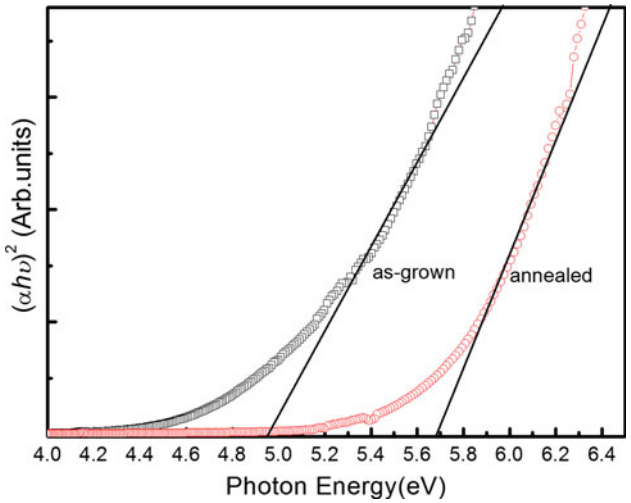

Fig. 6 Plot of $(\alpha hv)^2$ versus photon energy (hv) for as-grown and annealed Ga_2O_3 samples

optical band gap of the as-grown sample was 4.94 eV, which was approximately accord with the crystalline β-Ga_2O_3. However, the optical band gap of the annealed sample was increased to 5.68 eV, which was larger 0.74 eV than that of the as-grown samples. Similar phenomena were also observed by Yoshihiro Kokubun et al. [3]. Moreover, Yoshihiro Kokubun et al. detailed reported that the band gap increased with heat treatment temperature from 600 °C to 1,200 °C. And they still observed that the enlargement of the band gap was consistent with the peaks shift in the spectral response of photocurrent.

The 4.94 eV optical band gap of the as-grown sample was good agreement with the crystalline β-Ga_2O_3, but the 5.68 eV optical band gap of the annealed sample was apparently expanding. XRD patterns clearly presented that both samples were composed of polycrystalline and amorphous phases. The electron diffraction pattern confirmed the existence of the nanocrystal grains. AFM image indicated O_2 anneal treatment promoted the Ga_2O_3 films crystallization. PL spectrum of annealed sample showed obvious ultraviolet (UV) emission and broad red emission of Ga_2O_3. All experiment results confirmed the presence of the polycrystalline β-Ga_2O_3 and nanocrystal grains embedding in the amorphous Ga_2O_3. As well known, optical band gap could be increased by reducing the size of nanocryatal grains. Therefore, it was attributed to the quantum effect to broaden the optical band. The UV emission blue shift further revealed the quantum confinement effect. Thus, in PL spectra, the NBE emission was not observed. It might be the 224 nm laser energy was not so high to stimulate Ga_2O_3 NBE emission at 5.68 eV, which was 218 nm. In addition, the resistivity of the as-grown and annealed samples are very large and could not been measured by Hall Effect System (Accent, HL-5500).

4 Conclusion

Ga_2O_3 films were prepared on c-plane Al_2O_3 substrate by electron beam evaporation method with subsequent annealing treatment. XRD and electron diffraction patterns indicated that as-grown and annealed samples were polycrystalline β-Ga_2O_3 embedded in the amorphous Ga_2O_3. AFM images revealed that the anneal treatment promoted the film crystallization. Broad UV and red emissions were observed in PL measurement for annealed samples. The optical band gaps of as-grown and annealed sample were calculated to be 4.94 and 5.68 eV, respectively. The optical band gaps of annealed was larger than that of the bulk Ga_2O_3 material. It was attributed to the quantum size effect caused by the nanocrystal Ga_2O_3 grains. The blue shift of UV emission also confirmed the quantum confinement effect.

Acknowledgments This work was supported by national natural science foundation of China (NO.60976010, NO.61076045, NO.11004020), national high technology research and development program (863 program) (NO.2011AA03A102), the fundamental research funds for the central universities (NO.DUT12LK22, DUT11LK43, DUT11RC(3)45), the research fund for the doctoral program of higher education (No. 20110041120045), the open fund of the state key laboratory of functional materials for informatics.

References

1. H.H. Tippins, Phys. Rev. **140**, A316 (1965)
2. Y. Lv, J. Ma, W. Mi, C. Luan, Z. Zhu, H. Xiao, Vacuum **86**, 1850–1854 (2012)
3. Y. Kokubun, K. Miura, F. Endo, S. Nakagomi, Appl. Phys. Lett. **90**, 031912 (2007)
4. J.L. Zhao, X.W. Sun, H. Ryu, S.T. Tan, IEEE T. Electron Dev. **58**, 1447 (2011)
5. M. Higashiwaki, K. Sasaki, A. Kuramata, T. Masui, S. Yamakoshi, Appl. Phys. Lett. **100**, 013504 (2012)
6. M. Orita, H. Ohta, M. Hirano, H. Hosono, Appl. Phys. Lett. **77**, 4166 (2000)
7. R. Suzuki, S. Nakagomi, Y. Kokubun, Appl. Phys. Lett. **98**, 131114 (2011)
8. P. Feng, J.Y. Zhang, Q.H. Li, T.H. Wang, Appl. Phys. Lett. **88**, 153107 (2006)
9. E.G. Víllora, K. Shimamura, K. Kitamura, K. Aok, Appl. Phys. Lett. **88**, 031105 (2006)
10. M. Fleischer, W. Hanrieder, H. Meixner, Thin Solid Films **190**, 93 (1990)
11. S.L. Ou, D.S. Wuu, Y.C. Fu, S.P. Liu, R.H. Horng, L. Liu, Z.C. Feng, Mater. Chem. Phys. **133**, 700 (2012)
12. L. Kong, J. Ma, C. Luan, W. Mi, Y. Lv, Thin Solid Films **520**, 4270 (2012)
13. S. Penner, B. Klötzer, B. Jenewein, F. Klauser, X. Liu, E. Bertel, Thin Solid Films **516**, 4742 (2008)
14. Y.D. Liu, X.C. Xia, H.W. Liang, H.Z. Zhang, J.M. Bian, Y. Liu, R.S. Shen, Y.M. Luo, G.T. Du, J. Mater, Sci –Mater. Electron **23**, 542 (2012)
15. H.W. Kim, S.H. Shim, Thin Solid Films **515**, 5158 (2007)
16. J. Zhang, F. Jiang, Chem. Phys. **289**, 243 (2003)
17. C.H. Liang, G.W. Meng, G.Z. Wang, Y.W. Wang, L.D. Zhang, Appl. Phys. Lett. **78**, 3202 (2001)
18. M.B. Sahana, C. Sudakar, A. Dixit, J.S. Thakur, R. Naik, V.M. Naik, Acta Mater. **60**, 1072 (2012)
19. Kuo-Feng Lin, Hsin-Ming Cheng, Hsu-Cheng Hsu, Li-Jiaun Lin, Wen-Feng Hsieh, Chem. Phys. Lett. **409**, 208 (2005)
20. X.C. Wu, W.H. Song, W.D. Huang, M.H. Pu, B. Zhao, Y.P. Sun, J.J. Du, Chem. Phys. Lett. **328**, 5 (2000)
21. L. Binet, D. Gourier, J. Phys. Chem. Solids **59**, 1241 (1998)
22. Y.P. Song, H.Z. Zhang, C. Lin, Y.W. Zhu, G.H. Li, F.H. Yang, D.P. Yu, Phys. Rev. B **69**, 075304 (2004)
23. Y.B. Li, T. Tokizono, M. Liao, M. Zhong, Y. Koide, I. Yamada, J–.J. Delaunay, Adv. Funct. Mater. **20**, 3972 (2010)